

A Study on the Structure and Thermal Property of Co²⁺-Exchanged Zeolite A

Jong-Yul Park

Department of Chemistry, Pusan National University, Pusan 609-735 Received August 25, 1990

Theoretical calculations on the stabilization energies of framework atoms in hydrolysed Co(II)-exchanged zeolite A were made using some potential energy functions and optimization program.

The protons which are produced by hydrolysis of [Co(H₂O)_n]²⁺ ion in large cavity showed a tendency to attack the framework oxygen atom O(1) preferentially, and the oxygen atom O(4) within OH⁻ ion was coordinated at Al atom. The weakness of bonds between T(Si, Al) and oxygen by attack of proton and too large coordination number around small aluminum atom will make the framework of Co(II)-exchanged zeolite A more unstable. The stabilization energy of Co₄Na₄-A framework (-361.57 kcal/mol) was less than that of thermally stable zeolite A(Na₁₂-A: -419.68 kcal/mol) and greater than that of extremely unstable Ba(II)-exchanged zeolite A(Ba₆-A: -324.01 kcal/mol). All the data of powder X-ray diffraction, infrared and Raman spectroscopy of Co(II)-exchanged zeolite A showed the evidence of instability of its framework in agreement with the theoretical calculation. Three different groups of water molecules are found in hydrated Co(II)-exchanged zeolite A: W(I) group of water molecules having only hydrogen-bonds, W(II) group water coordinated to Na⁺ ion, and W(III) group water coordinated to Co(II) ion. The averaged interaction energy of each water group shows the decreasing order of W(III)>W(II)>W(I).

Introduction

Zeolites are important materials which are well known for its wide industrial applications as catalysts, molecular sieves, ion-exchangers, adsorbents, and other usages.

Zeolite A is one of aluminosilicates with composition of Na₁₂[Al₁₂O₂₄Si₁₂O₂₄] \cdot 27H₂O, and its framework is made up with sharing of each oxygen atom at apex of SiO₄ and AlO₄ tetrahedra.

The wide usages of zeolites arise from its specific chemical environment and characteristic structure having interconnected channels, windows, and cavities which make zeolite framework have great void volume and large surface area.

Zeolite A which was exchanged with K⁺, Mg(II), Ca(II), Zn(II), and Mn(II) are stable by dehydration upon heating^{1,2}, but some divalent cation-exchanged zeolite A, such as Ba(II) or Ni(II)-exchanged zeolite A shows a great thermal instability by dehydration.^{1,5}

Since the structural changes such as degradation or decomposition will lead the zeolite framework lose their characteristic properties, the study on the structure and stability of zeolite framework have been an important area of research.

The most definite structural informations are obtained from single crystal X-ray and neutron diffraction.

Infrared⁶, Raman⁷, EPR⁸, and solid-state NMR spectroscopy⁹ also provide useful informations on zeolite structure.

Paul E. Riley and Karl Seff¹⁰ reported the hydrolysed structure of Co(II)-exchanged zeolite A (Co₄Na₄-A) by the single crystal X-ray diffraction.

But the energetic study on the framework stability of Co(II)-exchanged zeolite A with relation to hydrolysis effect has not been made yet.

In this work, three kind of Co(II)-exchanged zeolite A (Co_xNa_{12-2x}-A; x=1, 2, 4) having different composition are prepared and the structural changes and thermal stabilities of these samples will be investigated by means of powder

X-ray diffraction, thermal analysis, infrared, and Raman spectroscopy.

The stabilization energy of framework atoms, protons, and water molecules within hydrolysed Co₄Na₄-A will be calculated by using some potential energy functions and computer programs developed by M. S. Jhon and K. T. No^{3,4}

The hydrolysis effects on the thermal stability of Co(II)-exchanged zeolite A will be discussed by the analysis of theoretical calculation and experimental data.

Experimental

The crystals of zeolite A(Na₁₂Al₁₂Si₁₂O₄₈ \cdot 27H₂O) were prepared by Charnell's method.¹¹ Ion exchange with 0.1 M Co(NO₃)₂ solution by static method yielded a pink-tan colored materials with stoichiometries of Co₁Na₁₀-A (A:Al₁₂Si₁₂O₄₈¹²⁻), Co₂Na₈-A, and Co₄Na₄-A.

A portion of each sample was heated at 100°C, 200°C, and 300°C for 5 hours respectively. Powder X-ray diffractograms within 2°<2θ<50° were obtained with Rigaku Geigerflex D/Max diffractometer with Ni-filtered CuK_α radiation.

Thermograms of differential scanning calorimeter (DSC) and thermogravimetric analysis (TGA) were recorded on a Rigaku Thermal Analyzer TAS 100 system. The Raman spectra in the region of 300-1200 cm⁻¹ were obtained by using radiation at 457.9 nm from a Spectra Physics Argon ion laser (Model 171), a Spex 1403 spectrometer, and a RCA C 3104 GaAs photomultiplier. The slit widths were typically 6 cm⁻¹ and laser powers at the samples were 50-100 mW. The mid-infrared spectra in the range of 400-1400 cm⁻¹ were recorded on a Mattson-Polaris TM spectrometer.

Calculation of Stabilization Energy

The geometry of the model compound, Co₄Na₄-A was taken from the X-ray crystallographic study¹⁰ and the potential parameters of the potential energy functions were refined

by the method which was used by M. S. Jhon and K. T. No³.

The total stabilization energy is expressed as sum of several potential energies.

$$V = V_d + V_{pot} + V_{d-r} + V_{T-O} \quad (1)$$

Electrostatic Energy (V_d). The net charges of the atoms are considered as point charge and electrostatic energy is given as

$$V = \sum_m \sum_{n>m} \delta_m \delta_n / r_{mn} \quad (2)$$

where δ_m and δ_n are the net charges of m th and n th atoms and r_{mn} is their interatomic distance. The net atomic charges are calculated using Huey's electronegativity set¹² and Sanderson's electronegativity equalization method¹³.

$$\sum_{i \in Na} \delta_i = -\delta_{Na} \quad (3)$$

$$a_i + b_j \delta_i = a_j + b_j \delta_j, \quad i, j = Na \quad (4)$$

where i and j represent T_1 , T_2 , O(1), O(2), O(3), and O(3) · T_1 , and T_2 are Si or Al atom.

The calculated net atomic charges are as follows; $\delta_{Na} = 0.625$, $\delta_{Co} = 1.250$, $\delta_{O(1)} = -0.4509$, $\delta_{O(2)} = -0.4548$, $\delta_{O(3)} = -0.4458$, $\delta_{O(3)'} = -0.4458$, $\delta_{T1} = 0.5861$, $\delta_{T2} = 0.5861$.

Polarization Energy (V_{pot}). Polarization energy is given as follows;

$$V_{pot} = -1/2 \sum_i \alpha_i \left(\sum_{j \neq i} \vec{e}_{ij}^{(x)} \right)^2 + \left(\sum_{j \neq i} \vec{e}_{ij}^{(y)} \right)^2 + \left(\sum_{j \neq i} \vec{e}_{ij}^{(z)} \right)^2 \quad (5)$$

where α_i is the atomic polarizability of the i th atom and $\vec{e}_{ij}^{(x)}$ is the electrostatic field in the X-direction at the i th atomic position created by j th atom.

Harmonic Potential Energy (V_{T-O}). The harmonic function for T-O bonds is as follows,

$$V_{T-O} = 1/2 \sum_i \sum_{j>i} k_{ij} (r_{ij} - r_{ij}^0)^2 \quad (6)$$

where k_{ij} and r_{ij} are harmonic potential parameters and r_{ij} is an interatomic distance.

Dispersion and Repulsion Energy (V_{d-r}). A modified Kitaigorodskii potential function ($V_{d-r(9ii)}$)¹⁴ was used for the calculation of dispersion and repulsion energy.

$$V_{d-r(9ii)} = \sum_i \sum_{j>i} k_i k_j \{ -A/Z^6 + (1 - \delta_i / N_i^{val}) (1 - \delta_j / N_j^{val}) \} C \exp(-\alpha Z) \quad (7)$$

where $Z = R_{ij} / R_{ij}^{0'}$ and $R_{ij}^{0'} = [(2R_{ij}^{0*})(2R_{ij}^{0*})]^{1/2}$ where R_{ij}^{0*} and $R_{ij}^{0'}$ are the van der Waals radii of atom i and j . The parameter A , C , and α are 0.214 kcal/mol, 47000 kcal/mol, and 12.35, respectively. k_i and k_j are multiplication factor of atom i and j . The k values¹⁵ used in this work are $k_H = 1.00$, $k_O = 1.36$, $k_T = 2.10$, $k_{Na} = 2.86$, and $k_{Co} = 3.00$. δ_i is net charge of atom i , and N_i^{val} is the number of valence electron of neutral atom i . This modification scheme is also applied to the case of hydrogen bond.

The stabilization energies and positions of framework atoms, ions, and water molecules were obtained by the optimization of total energies interacting between all i th and j th atoms within 216 unit cells of Co_4Na_4 -A. The optimization program, VA10A developed by Fletcher¹⁶ was used in this work. For the calculation of the stabilization energies of water molecules in hydrated state, only electrostatic energy, polarization energy and dispersion-repulsion energy were considered. The stabilization energy of framework atoms and protons according to the binding site of proton in hydrolyzed Co_4Na_4 -A are listed in Table 1.

Table 2 shows the optimized positions and stabilization energies of protons in hydrolysed Co_4Na_4 -A. The framework energies of some of the divalent cation-exchanged zeolite A are listed in Table 3.

Results and Discussion

Recently, crystallographic studies have shown that some kinds of hydrated cations within zeolite promote an extensive hydrolysis, and this hydrolysis makes zeolite framework unstable.^{10,18} But no energetic investigations of the hydrolysis effect on the stability of zeolite framework have been made yet.

Table 1 shows that the stabilization energy of framework

Table 1. The Stabilization Energies of Framework Atoms and Protons of Hydrolysed Co_4Na_4 -A According to the Binding Site of Proton

Framework atom	Stabilization energy (kcal/mol) binding site of proton				
	Hydrated state			Dehydrated state	
	O(1)	O(2)	O(3)	O(3)'	O(1)
T_1	-200.57	-218.21	-248.95	-205.66	-191.80
T_2	-200.33	-217.97	-248.61	-205.38	-191.94
O(1)	-2.89	41.44	65.91	33.55	-10.96
O(2)	10.55	6.64	49.28	22.42	11.98
O(3)	11.71	17.86	29.23	-0.97	10.58
O(3)'	11.67	17.81	29.18	-1.01	10.57
$E_{(f,w)}$	-369.86	-352.43	-323.96	-357.05	-361.57
$E_{(9H^+)}$	-195.50	-155.07	-146.25	-173.42	-152.26
$E_{(tot)}$	-565.36	-507.50	-470.21	-530.47	-513.83

$E_{(f,w)}$: stabilization energy of framework, $E_{(9H^+)}$: total stabilization energy of 9 protons in unit cell, $E_{(tot)} = E_{(f,w)} + E_{(9H^+)}$.

Table 2. The Optimized Positions and Stabilization Energies of Protons in Hydrolysed Co₄Na₄-A

No. H ⁺	Hydrated state				Dehydrated state			
	x (Å)	y (Å)	z (Å)	Energy ^a	x (Å)	y (Å)	z (Å)	Energy ^a
1	-0.710	-5.031	2.866	-22.87	-0.719	-4.904	3.281	-18.32
2	-2.285	0.674	5.566	-20.87	-2.668	-0.651	5.395	-16.92
3	-4.477	-1.479	0.219	-27.24	-4.422	-1.633	0.240	-20.37
4	0.769	-3.959	-3.029	-18.31	0.788	-4.138	-2.952	-18.92
5	3.106	0.525	-4.607	-17.10	3.054	0.523	-4.521	-10.32
6	5.349	-2.108	0.372	-18.00	5.351	-2.135	0.000	-15.63
7	0.105	6.359	-4.334	-18.83	-0.151	5.890	-4.303	-14.65
8	-1.159	-1.859	-7.985	-22.80	-1.301	-1.658	-7.177	-14.81
9	-6.195	4.351	-0.041	-24.35	-6.194	4.353	-0.031	-22.32
<i>E_{tot}</i>				-195.50				-152.26

^a Unit of energy: kcal/mol.

Table 3. The Stabilization Energies of Framework Atoms of Zeolite A and Some of the Cation-Exchanged Zeolite A

Framework atom	Stabilization energy (kcal/mol)				
	Na ₁₂ -A ¹⁶	Ca ₆ -A ¹⁶	Mn _{4.5} Na ₃ -A ²	Co ₄ Na ₄ -A ^e	Ba ₆ -A ³²
T ₁	-163.47	-179.79	-197.95	-191.80	-218.14
T ₂	-163.87	-179.52	-186.21	-191.94	-205.11
O(1)	-18.90	-3.47	8.57	-10.96	8.95
O(2)	-25.82	-17.04	3.68	11.98	34.15
O(3)	-23.61	-5.13	1.94	10.58	32.59
O(3)'	-23.61	11.93	-8.07	10.57	23.55
<i>E_{tot}</i>	-419.68	-373.02	-378.04	-361.57	-324.01

^eThis work.

atoms and protons are dependent on the binding site of proton.

While protons are bound to framework oxygen atom O(1), the framework atoms and 9 protons of Co₄Na₄-A showed the greatest stabilization energies in the both cases of hydrated state (-565.36 kcal/mol) and dehydrated state (-513.83 kcal/mol) respectively.

This suggests that the most preferable binding site of protons might be the O(1).

The dependence of stabilization energy on the binding site of proton may arise from the different chemical environment of each framework oxygen atom.

It is not surprising that protons tend to seek O(1) atoms preferentially, considering that cations are located more closely to O(3) and O(2) than O(1).

Table 1 also shows that the total stabilization energy, *E_{tot}*, of framework atoms and protons in dehydrated Co₄Na₄-A is less than that of hydrated Co₄Na₄-A by 51.83 kcal/mol.

The difference in energy between above two states is originated mainly from the decreased stabilization energy of protons (by 43.24 kcal/mol) and partly from the instability of framework (by 8.29 kcal/mol) by the loss of hydrogen bond energy upon dehydration.

The optimized positions and stabilization energies of protons are listed in Table 2. The stabilization energies of framework of dehydrated zeolite A and some of divalent cation-exchanged zeolite A are listed in Table 3.

The decreasing order of stabilization energy of framework is Na₁₂-A: -419.68 kcal/mol > Mn_{4.5}Na₃-A: -378.04 kcal/mol > Ca₆-A: -373.02 kcal/mol > Co₄Na₄-A: -361.57 kcal/mol > Ba₆-A: -324.01 kcal/mol.

Table 3 shows clearly that divalent cation-exchanged zeolite A are less stable than zeolite A (Na₁₂-A). Especially Ba₆-A³² has the least stabilization energy which is in agreement with crystallographic instability.⁵

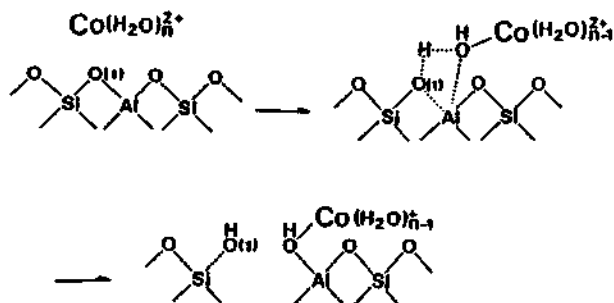
Y. Kim *et al.*⁵ attributed the instability of Ba(II) ion-exchanged zeolite A to its large ionic size (*r*_{Ba(II)} = 1.34 Å).

While dehydration occurs, Ba(II) ion can not approach more closely to the center of 6-ring window which is preferable site for cations in dehydrated state of cation-exchanged zeolite A because of its large ionic radius.⁵

Then some of Ba(II) ions under this situation moves to larger site, 8-ring window. Since Ba(II) ion at this site has only three coordinations with framework oxygen, they might try to seek the normal coordination number 6 by demolishing zeolite framework.⁵

In spite of the small size of Co(II) ion (*r*_{Co(II)} = 0.745 Å³⁴) the Co(II) ion-exchanged zeolite A shows a considerable decrease in framework stabilization energy. This suggests that the instability of Co₄Na₄-A arise from another different process.

Uytterhoeven *et al.*, reported that the strong Brønsted acid H⁺ and [M^{m+}(H₂O)_{n-1}(OH)]^{(m-1)+} species of ion can be produced by dissociation of water molecules which are coordi-



Scheme 1.

nated to the specific cation with high electric field, and these ions attack the anionic framework to give Si-OH group.

The structural analysis¹⁰ showed that three water molecules which are coordinated to each Co(II) ion in α -cage are hydrolysed.

The hydrolysis effects on the stability of zeolite framework might be as follows;

The one is that the protons which are produced and accumulated in zeolite attack the framework oxygen, O(1). This attacking of proton will make the bonds between T₁(T₂) and oxygen more weakened.

This description above agreement with C. K. Hersh's report²⁰ that zeolite A is unstable at low pH; for instance, zeolite dissolves in static contact with a solution of pH=2.

Another one is the instability of framework due to too large coordination number of small aluminum atom by hydrolysis effect as shown at Scheme 1.

Scheme 1 shows the weakness of the bond between Al(Si) and the coordination of OH⁻ ion in the species of [Co(OH)₃(H₂O)]⁻.

The coordination of O(4) which forms Co(II)-O(4)-Al bridge makes small Al atom have coordination number 5.

The five coordinated aluminum will make the zeolite framework more unstable and will induce partial breakdown of zeolite framework, and then common coordination number (4) of Al will be restored. These two hydrolysis effects will reduce the framework interaction energy of Co(II)-exchanged zeolite A and will make the framework more unstable as shown in theoretical calculation (Table 3).

The decreased stability of Co(II)-exchanged zeolite A could be confirmed by X-ray diffraction, Raman, and infrared spectroscopy experiments.

Figure 1 shows that the intensities of X-ray diffraction peaks of unheated Co(II)-exchanged zeolite A decrease with the increasing contents of Co(II) ion and also with the increasing of heating temperature.

This X-ray diffraction data strongly suggests that the stability of zeolite framework is reduced and the crystal structure collapsed partially due to hydrolysis effect.

It is seen from Figure 1 that the framework stability of Co(II)-exchanged zeolite A is less than zeolite A, but greater than extremely unstable Ni(II)-exchanged zeolite A (Ni₅Na₂-A) which shows no X-ray diffraction peaks because of entire collapse of zeolite framework.

It is well known that infrared and Raman spectroscopy provide many useful information on the zeolite structure.^{6,21-25}

Flanigen *et al.*, assigned the vibration bands of zeolite fra-

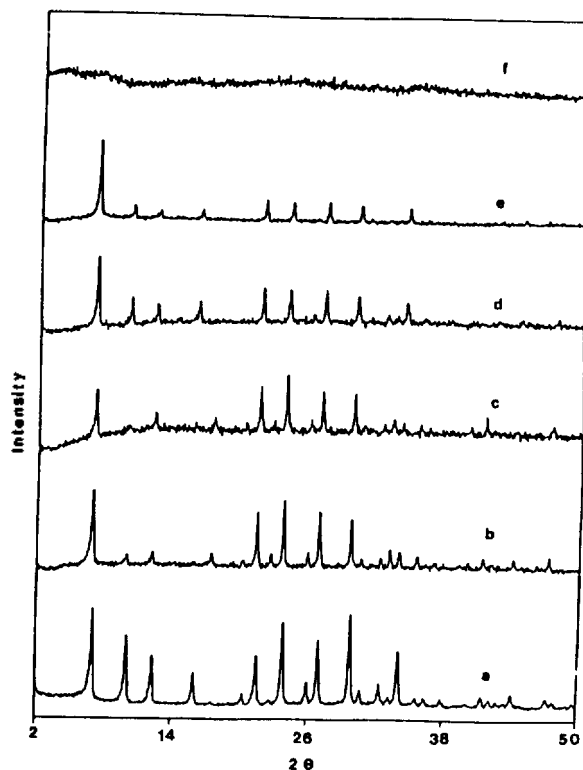


Figure 1. The X-ray diffraction patterns of Co₂Na_{12-2x}-A and Ni₅Na₂-A, a,b,c; unheated, d,e,f; heated, a: zeolite A, b: Co₂Na₁₀-A, c: Co₄Na₄-A, d: Co₄Na₄-A (200°C), e: Co₄Na₄-A (300°C), f: Ni₅Na₂-A (300°C).

mework as follows, 950-1250 cm⁻¹; asymmetric stretching vibration of TO₄, 650-720 cm⁻¹; symmetric stretching vibration of TO₄, 420-500 cm⁻¹; T-O bending vibration, 500-650 cm⁻¹; vibration of double ring (external linkage), 300-420 cm⁻¹; pore opening, 750-850 cm⁻¹; symmetrical stretching of external linkages, 1050-1150 cm⁻¹; asymmetric stretching of external linkage.

Figure 2 shows that all the samples of Co(II)-exchanged zeolite A show mid-infrared vibration bands of near 1000 cm⁻¹ (asymmetric stretching vibration of TO₄), 550 cm⁻¹ (vibration of double 4-ring), 460 cm⁻¹ (T-O bending vibration), 670 cm⁻¹ (symmetric stretching vibration of TO₄), and 820 cm⁻¹ (symmetric stretching of external linkage).

The intensity and shape of the band of external linkages (D4R) near 550 cm⁻¹ which is sensitive to the zeolite Structure gives useful information on the degradation of structure.

Many IR studies^{1,22,23,26,27} disclosed that the decrease of intensity and the broadening of the structure-sensitive bands indicate disruption and decomposition of framework and high concentration of defects.

Figure 2 shows that the intensities of all the bands of Co(II)-exchanged zeolite A are decreasing gradually according to the increasing content of Co(II) ion and also according to higher heating temperature. In the case of thermally unstable Ni₅Na₂-A, the structure-sensitive band (~550 cm⁻¹) disappeared completely by heating at 300°C.

This IR data also shows the evidence of reduced stability of Co(II)-exchanged zeolite A.

Recently, Raman spectroscopy has been extensively used to obtain information on the structure of various kinds of

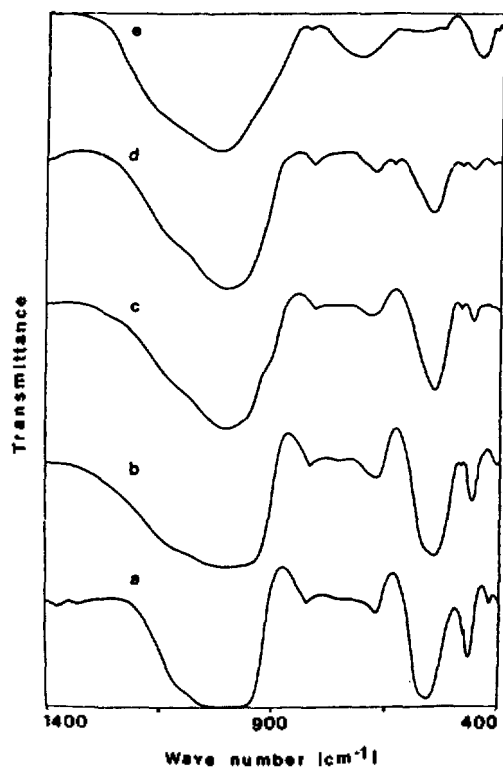


Figure 2. The infrared spectra of $\text{Co}_x\text{Na}_{12-2x}\text{-A}$ and $\text{Ni}_3\text{Na}_2\text{-A}$, a,b,c; unheated, d,e; heated, a: zeolite A, b: $\text{Co}_2\text{Na}_{10}\text{-A}$, c: $\text{Ni}_3\text{Na}_2\text{-A}$, d: $\text{Co}_4\text{Na}_4\text{-A}$ (3200°C), e: $\text{Co}_4\text{Na}_4\text{-A}$ (300°C).

zeolite.^{7,28-32} The Raman spectra of zeolite A and Co(II)-exchanged zeolite A ($\text{Co}_x\text{Na}_{12-2x}\text{-A}$) are shown in Figure 3.

Zeolite A shows strong Raman band at 491 cm^{-1} corresponding to SiO_4 deformation mode, very weak bands of Si-O stretching motions at 853 cm^{-1} , 971 cm^{-1} , and 1040 cm^{-1} , and very weak bands of Al-O stretching vibration in the range of $650\text{-}750\text{ cm}^{-1}$.

It can be seen from Figure 3 that according to the increasing content of Co(II) ion, the intensity of the structure-sensitive band at 491 cm^{-1} decrease gradually and the shape of this band becomes more broadened and shifts toward a little higher frequency.

The changes of Raman spectra also indicates the reduced stability of Co(II)-exchanged zeolite A.

All the data of X-ray diffraction and infrared, and Raman spectroscopy showed the evidence of instability of Co(II)-exchanged zeolite A and are agreed with the results of theoretical calculation on the framework energy.

The optimized positions and energies of 26 water molecules in hydrated $\text{Co}_4\text{Na}_4\text{-A}$ (Table 4) shows that there are three different kinds of water groups; W(I) group: water molecules which are located far apart from cation and make hydrogen bonds only with adjacent water molecules or framework oxygen atoms, W(II) group: water molecules coordinated to Na(I) ions, W(III) group: water molecules coordinated to Co(II) ions. The existence of some different kinds of water groups in hydrated state of zeolite A and cation-exchanged zeolite A was confirmed by other works^{2,4,17}.

The number of water molecules and average interaction energies of each water group are; W(I): $10\text{H}_2\text{O}$ (-7.59

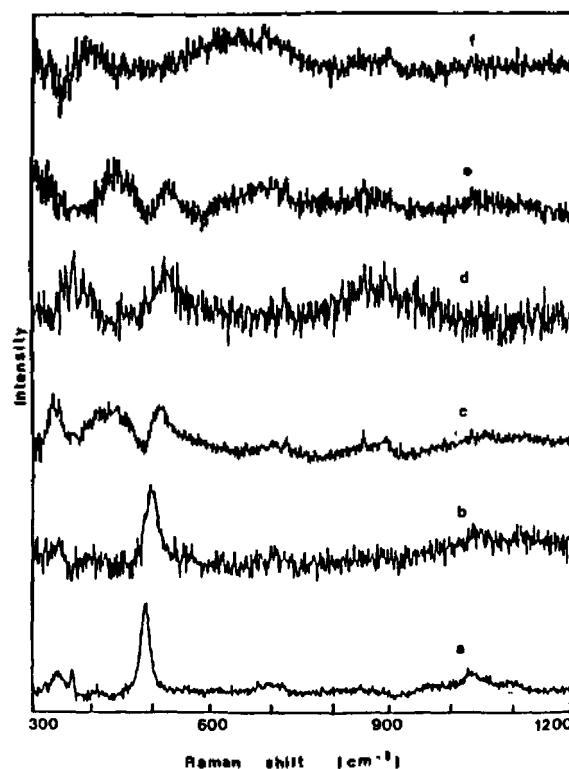


Figure 3. The Raman spectra of $\text{Co}_x\text{Na}_{12-2x}\text{-A}$, a,b,c,d; unheated, e,f; heated, a: zeolite A, b: $\text{Co}_2\text{Na}_{10}\text{-A}$, c: $\text{Co}_2\text{Na}_{10}\text{-A}$, d: $\text{Co}_4\text{Na}_4\text{-A}$ (200°C), e: $\text{Co}_4\text{Na}_4\text{-A}$ (100°C), f: $\text{Co}_4\text{Na}_4\text{-A}$ (300°C).

Table 4. The Average Stabilization Energies of Three Different Groups of Water Molecules in Hydrated $\text{Co}_4\text{Na}_4\text{-A}$

Water group	Tm ^a of DSC (°C)	Number of water molecules (per unit cell)	Average stabilization energy (kcal/mol) (by calculation)
W(I)	79.1	10	-7.59
W(II)	134.2	10	-10.22
W(III)	220.5	6	-18.57
Total stabilization energy of water molecules by calculation;			-289.50
Dehydration energy per unit cell by DSC:			-269.26

^aMaximum deflection temperature.

kcal/mol), W(II): $10\text{H}_2\text{O}$ (-10.2 kcal/mol), W(III): $6\text{H}_2\text{O}$ (-18.57 kcal/mol).

The total stabilization energy of 26 water molecules (-289.50 kcal/mol) by calculation is approximately agreed with the dehydration energy (269.26 kcal/mol) determined by differential scanning calorimeter.

Figure 4 shows that there are three smooth steps of TGA curve and corresponding three endothermic peaks of DSC at the temperatures of near 79°C , 134°C , and 220°C respectively.

According to the increase of Co(II) ion content which is accompanied with the decrease of Na ion, the third endothermic peak at 220°C increases while the second peak decrease gradually. This means that the second DSC peak (134°C) is

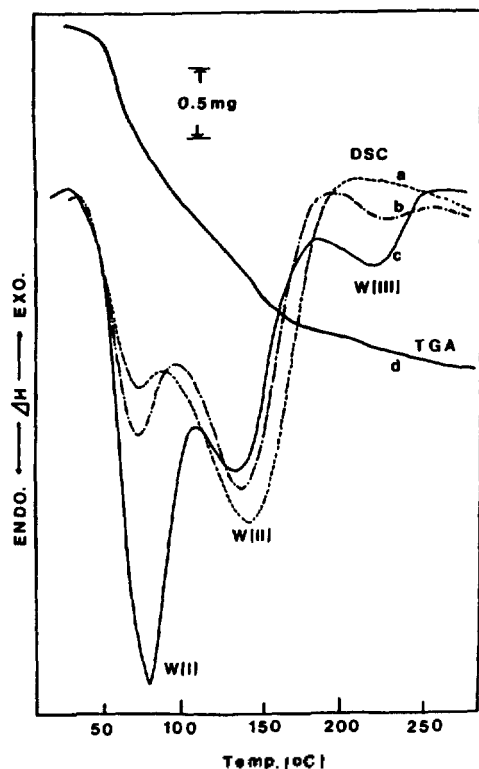


Figure 4. The TGA and DSC thermograms of $\text{Co}_x\text{Na}_{12-2x}\text{-A}$, a, b, c; DSC, a: $\text{Co}_1\text{Na}_{10}\text{-A}$, b: $\text{Co}_2\text{Na}_8\text{-A}$, c: $\text{Co}_4\text{Na}_4\text{-A}$, d: TGA of $\text{Co}_4\text{Na}_4\text{-A}$.

due to the dehydration of W(II) group of water bound to Na ion, and third peak (220°C). corresponds to the dehydration of W(III) group of water which coordinated to Co(II) ion.

The increase of first peak (79°C) in accordance with the increase of Co(II) ion content may arise from the increase of the water molecules which are bound weakly by hydrogen bonds in α -cage or the water molecules which are simply adsorbed at the surface of Co(II)-exchanged zeolite A.

Co(II) ion with high electric field can contract the hydration sphere strongly, and will make more space to accommodate weakly bound water molecules in α -cage.

By the analysis of TGA and calculated data, the first DSC endo peak could be assigned to the dehydration of W(I) group of water molecules.

Acknowledgement. I acknowledge the financial supports for this work partly from the Professor Training Program of the Korean Government, 1989 and partly from the Basic Science Institute Program, Ministry of Education, 1989. I thank professor Prabir K. Dutta at Ohio State University for providing facilities of analytical instruments.

References

1. F. Wolf, H. Fuertig, and Tonind, *Ztg. Keram. Rundschau*, **90**, 310 (1966).
2. J. Y. Park, Y. Kim, U. S. Kim, and S. G. Choi, *J. Kor. Chem. Soc.*, **33**, 623 (1989).
3. M. S. Jhon, K. T. No, J. S. Kim, Y. Y. Huh, and W. K. Kim, *J. Phys. Chem.*, **91**, 740 (1987).
4. K. T. No and M. S. Jhon, *J. Kor. Chem.*, **374** (1979).
5. Y. Kim, V. Subramanian, R. L. Firror, and K. Seff, *ACS Symposium Series No. 135, Adsorption and Ion Exchange with Synthetic Zeolites*, 137 (1980).
6. E. M. Flanigen, H. Khtami, and H. A. Szymanski, *Adv. Chem. Series*, **101**, 301 (1971).
7. P. K. Dutta and B. D. Barco, *J. Phys. Chem.*, **89**, 1861 (1989).
8. R. A. Schoonheydt, I. Vaesen, and H. Leeman, *J. Phys. Chem.*, **93**, 1515 (1989).
9. R. Janssen, G. A. H. Tizink, W. S. Veeman, Th. L. M. Maesen, and J. F. Van Lent, *J. Phys. Chem.*, **93**, 899 (1989).
10. P. E. Riley and K. Seff, *J. Phys. Chem.*, **79**, 1594 (1975).
11. J. F. Charnell, *J. Cryst. Growth*, **8**, 291 (1971).
12. J. E. Hueey, *J. Phys. Chem.*, **69**, 3284 (1965).
13. R. T. Sanderson, *J. Phys. Educ.*, **31**, 2 (1945).
14. J. Gaillet, P. Claverie, and B. Pullman, *Acta Crystallogr.*, **B32**, 2740 (1976).
15. M. J. Huron and P. Claverie, *J. Phys. Chem.*, **76**, 2123 (1972).
16. R. Fletcher, *Fortran subroutines for minimization by quasi-Newton methods AERE report R 7125* (1974).
17. J. Y. Park, Y. Kim, U. S. Kim, and S. G. Choi, *J. Kor. Chem. Soc.*, **33**, 357 (1989).
18. R. L. Firor and K. Seff, *J. Phys. Chem.*, **82**, 1650 (1978).
19. J. B. Uytterhoeven, R. A. Schoonheydt, B. V. Liengme, and W. K. Hall, *J. Catal.*, **13**, 425 (1969).
20. C. K. Hersh, "Molecular Sieves", Reinhold, New York, N. Y., p. 55, 1961.
21. P. A. Jacobs and J. B. Uytterhoeven, *J. Phys. Soc. Faraday Trans*, **69**, 359, 373 (1973).
22. O. Lahodny-Sârc and J. L. White, *J. Phys. Chem.*, **75**, 2408 (1971).
23. J. A. Rabo, "Zeolite Chemistry and Catalysis, ACS Monograph", **171**, p. 80-113 (1976).
24. W. M. Butler, C. L. Angell, W. Mcallister, and W. M. Risen, Jr., *J. Phys. Chem.*, **81**, 2061 (1977).
25. J. Gobder, M. D. Baker, and G. A. Ozin, *J. Phys. Chem.*, **93**, 1409 (1989).
26. F. Wolf, H. Fuertig, and V. Haedicke, *Chem. Tech. (Berlin)*, **18**, 524 (1966).
27. A. A. Kubasov, K. V. Topchieva, and A. N. Ratov, *Russ. J. Phys. Chem.*, **47**, 1023 (1973).
28. P. K. Dutta, D. C. Shieh, and M. Puri, *Zeolites*, **8**, 306 (1988).
29. P. K. Dutta and B. D. Barco, *J. Chem. Soc., Chem. Commun.*, 1297 (1985).
30. P. K. Dutta and B. D. Barco, *J. Phys. Chem.*, **92**, 354 (1988).
31. F. Roozeboom and H. E. Robson, *Zeolites*, **3**, 321 (1983).
32. P. K. Dutta and M. Puri, *J. Phys. Chem.*, **91**, 4329 (1987).
33. S. G. Choi, Thesis of Ph. D., Pusan National University (1990).
34. N. H. Heo, W. Cruz-Patalinghug, and K. Seff, *J. Phys. Chem.*, **90**, 3931 (1986).